2011 American Control Conference
on O'Farrell Street, San Francisco, CA, USA
June 29 - July 01, 2011

Battery Swapping Modularity Design for Plug-in HEVs Using the Augmented Lagrangian Decomposition Method

Shifang Li, Ilya V. Kolmanovsky and A. Galip Ulsoy

Abstract—**A distributed supervisory controller is proposed to achieve battery component swapping modularity (CSM) for a plug-in hybrid electric vehicle (PHEV). The CSM permits to distribute a part of the controller to the battery module such that the PHEV can use a range of batteries while providing optimal fuel economy. A feedback based controller is proposed to facilitate battery CSM design. The control strategy is to optimize fuel economy and driving performance in terms of wheel power tracking error, while smoothing engine power and sustaining battery state of charge. The distributed controller with battery CSM is obtained by solving a bi-level optimization problem via the augmented lagrangian decomposition method. The simulation results demonstrate that battery CSM can be achieved without compromising fuel economy.**

I. Introduction

Plug-in hybrid electric vehicles (PHEVs) enable the transportation sector to access lower-cost, cleaner, and renewable energy from the electric grid [1]. One main barrier to the commercialization of PHEVs is the cost of the batteries. Increasing the battery energy capacity from 20 to 40 miles of all electric range provides an extra 15% reduction in fuel consumption, but it also nearly doubles the incremental cost [2]. It is thus beneficial to investigate the design of the PHEV which enables different batteries to be applied to the same vehicle. As battery technology advances, the vehicle can be easily upgraded with newer batteries (e.g., batteries with higher energy capacity).

From the perspective of component swapping modularity (CSM) [3], the battery component is swappable if: (1) the vehicle configurations before and after battery change operate at their corresponding optimal performance, (2) re-work in terms of software and controller calibration is limited to the battery component only, when battery change occurs. With CSM, the battery becomes a "plug and play" component. The interest in plug and play control has been steadily increasing, e.g. [4]. Opportunities to implement plug and play control systems are emerging in systems consisting of smart components connected by bi-directional communication networks [5].

Two design methods have been proposed to realize CSM in control systems. The 3-step method, which yields the distributed controllers with CSM by matching with a pre-computed centralized controller, has been developed and applied to automotive problems in [3, 6-8]. The direct method proposed in [9] generates the distributed controllers by solving a bi-level optimization problem. The direct method is applicable to nonlinear, as well as linear, controllers and can improve CSM compared to the 3-step method [9]. In this paper, to achieve battery CSM, a bi-level optimization problem is solved using the augmented lagrangian decomposition (ALD) method [10]. The ALD method is more complex, but provides more design freedom for each inner stage problem, compared to the direct method.

Current supervisory controllers for PHEVs all have centralized architectures, see [11]. A typical PHEV operates in a charge depleting (CD) mode before the battery state of charge (SoC) decreases to a certain value, then it switches to a charge sustaining (CS) mode. In the CD mode, the battery provides the propulsion energy, while the engine is used to satisfy the transient load demand beyond the power capacity of the battery. In the CS mode, the PHEV operates similarly to a conventional series hybrid electric vehicle, and the battery assists the engine in transients. In this paper, we treat the CD mode control strategy as given, and focus on CS mode control for battery CSM design.

The control strategies proposed for HEVs can be applied to the CS mode controller design for PHEVs. Examples of such strategies include rule based [12], and optimization based control, (e.g., equivalent consumption minimization strategy [13], stochastic and deterministic dynamic programming [14, 15]). Feedback–based controllers have also been developed for load following while smoothing engine power [16]. The feedback controller synthesized from model predictive control to smooth engine power was experimentally evaluated and showed improved fuel economy compared to two baseline strategies [17].

In this paper, a novel feedback-based controller for the CS mode is proposed to facilitate battery CSM design. The controller gains are generated over the EPA US06 cycle to minimize fuel consumption and vehicle power tracking error, while sustaining battery state of charge. Then, part of the centralized controller is distributed into the battery module such that only the controller gains distributed into the battery module are dependent on the battery parameters. The distributed controller gains, which enable battery CSM, are obtained by solving a bi-level optimization problem numerically using the ALD method. The simulation results demonstrate that battery CSM in PHEVs can be achieved without compromising fuel economy.

Shifang Li (corresponding author) and A. Galip Ulsoy are with the Department of Mechanical Engineering, University of Michigan, Ann Arbor, MI, 48109-2125. email: {sfli, ulsoy}@umich.edu
Ilya V. Kolmanovsky is with the Department of Aerospace Engineering, University of Michigan, Ann Arbor, MI, 48109-2140.
email: {ilya@umich.edu}

The paper is organized as follows: Section II presents the vehicle model used in this analysis. Section III explains the centralized supervisory controller. Section IV presents the distributed supervisory controller which enables battery CSM. Section VI gives the conclusions.

II. VEHICLE MODEL

The control-oriented vehicle model is presented in this section. The model inputs are the wheel power command, $P_{w,cmd}$, and the reference battery SoC, soc_r. The system outputs are the actual wheel power delivered, P_w, accumulated engine fuel consumption, *fuel*, and actual battery SoC, *soc*. A diagram of a series PHEV is illustrated in Fig. 1. The supervisory controller generates the engine /generator power command and the battery power command. The wheels are driven by the electric motor. The battery is being charged, when the battery power P_b is negative.

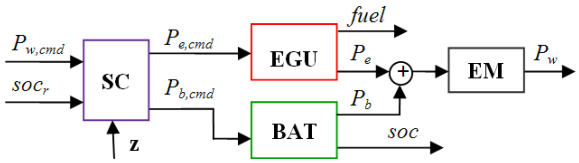

SC – supervisory controller
EGU – internal combustion engine and generator unit
BAT – battery
EM – electric machine
z – feedback state vector

Fig. 1. Diagram of the hybrid electric vehicle.

The key component sizes of the nominal vehicle configuration are listed in TABLE I. This PHEV is representative of current designs, such as the 2011 Chevrolet Volt. In the sequel, the controller will be designed for CSM of four batteries with different energy capacity (and different all electric range capability) for the same vehicle.

TABLE I
NOMINAL VEHICLE CONFIGURATION

PHEV	All Electric Range (AER) (mile)	30
Engine	Engine Power (kW)	50
Generator	Generator Power (kW)	50
Battery	Battery Capacity (kWh)	12
	Battery Maximum Power (kW)	110
Motor	Motor Power (kW)	110
Vehicle	Vehicle Weight (kg)	1680

The engine is modeled as a static fuel consumption map as shown in Fig. 2 [18]. Given a required power level, there is usually a unique pair of engine torque and speed which achieves minimum fuel consumption. The optimal operating points line (OOP-Line) is defined as the curve on which the fuel consumption is minimized for each power level [16].

The motor and generator are modeled using a constant mean efficiency $\eta_m = \eta_g = 0.85$, to linearize the powertrain system.

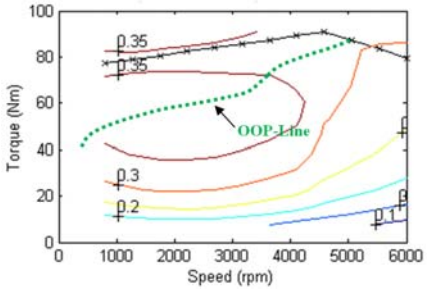

Fig. 2. Engine fuel consumption map (g/W/h).

The battery efficiency is assumed to be $\eta_b = 0.9$. The battery is modeled as an integrator with parameter B_s [17].

$$\frac{d\Delta soc}{dt} = -B_s P_{b,cmd} \tag{1}$$

where $\Delta soc = soc_r - soc$.

Here we consider four candidate batteries for CSM design. As a benchmark comparison, in the Chevrolet Volt, the energy capacity of the Lithium-ion battery is 16 kWh, which can provide about 40 mile all electric range with a battery weight of 175 kg. Four batteries with similar characteristics are scaled to have the parameters in TABLE II. Note that as B_s increases, the all-electric range, battery energy capacity and battery weight decreases.

TABLE II
BATTERY PARAMETERS

#	Battery number	1	2	3	4
AER (mile)	All-electric range	60	45	30	15
E_b (kWh)	Battery energy capacity	24	18	12	6
B_s (e-5)	Battery Parameter	1.29	1.71	2.57	5.14
W_b (kg)	Battery weight	263	197	131	66

III. CENTRALIZED SUPERVISORY CONTROLLER

The control strategy ensures gradual operation of the engine along the steady-state OOP Line while sustaining the battery charge. The goal for gradual (i.e. slow varying) operation of the engine is based on the perspective that aggressive engine transients and engine operation away from the OOP-Line may degrade fuel economy and emissions [16, 17]. In this paper, we only consider the power flows in this system. Lower level controllers, which realize the power demand from the components, are not considered.

A. Feedback-based controller

The vehicle model is augmented with two integrators to regulate the battery SoC and to eliminate wheel power tracking error during steady state. The resulting three states of the closed loop system are:

$$z_1 = \Delta soc = soc_r - soc \tag{2}$$

$$z_2 = \int (\Delta soc)dt = \int (soc_r - soc)dt \tag{3}$$

$$z_3 = \int (P_{w,cmd} - P_e - P_b)dt \tag{4}$$

where z_1 represents the deviation of battery SoC, *soc*, from the reference value, soc_r; z_2 represents the integral error of battery SoC; and z_3 represents the integral wheel power tracking error. The actual wheel power, P_w, equals the summation of the engine power P_e and the battery power P_b.

The control algorithm includes state feedback, feed-forward control and information exchange between the engine power command and the battery power command.

$$P_{e,cmd} = \mathbf{K_1}\,\mathbf{z} + n_1\,P_{w,\,cmd} + k_e P_{b,cmd} \tag{5}$$

$$P_{b,cmd} = \mathbf{K_2}\,\mathbf{z} + n_2\,P_{w,\,cmd} + k_b P_{e,cmd} \tag{6}$$

where $\mathbf{z} = [z_1\ z_2\ z_3]^{\mathrm{T}}$ is the state vector; $\mathbf{K_1} = [k_1\ k_2\ k_3]$ and $\mathbf{K_2} = [k_4\ k_5\ k_6]$ are state feedback gain vectors; n_1 and n_2 are feed-forward gains; k_e and k_b are controller gains that represent the information exchange.

The regulation of battery SoC should be slow to allow the battery to augment the engine in transients, while the wheel power tracking should be fast and accurate for good driving performance and safety. In order to achieve different convergence rates for different states, we employ eigen-structure assignment [19] to decouple the state z_3 from the other two states, z_1 and z_2, which are related to battery SoC. For desired closed loop poles p_1, p_2 and p_3, we obtain equations (7) relating the controller gains and the poles:

$$\begin{aligned} k_1 &= -\frac{(p_1+p_2)\eta_b}{B_s\eta_g}\ ,\ k_2 = \frac{p_1 p_2 \eta_b}{B_s\eta_g} \\ k_3 &= -\frac{p_3}{\eta_m\eta_g}\ ,\ k_4 = -\frac{k_1\eta_g}{\eta_b} \\ k_5 &= -\frac{k_2\eta_g}{\eta_b}\ ,\ k_6 = 0 \end{aligned} \tag{7}$$

The six feedback gains are uniquely determined by the desired closed loop poles for a specific vehicle configuration with battery parameter B_s. Note that k_6 equals 0, k_4 and k_5 are determined by k_1 and k_2, respectively. Therefore, we have three independent feedback gains, k_1, k_2 and k_3 to optimize.

B. Optimization of the controller gains

The aggressive driving cycle of EPA US06 (see Fig. 3) is chosen to generate the controller gains through optimization.

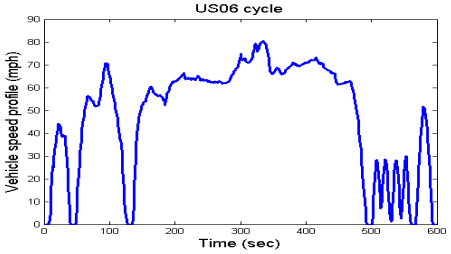

Fig. 3. EPA US06 driving cycle

Since we do not consider regenerative braking in this paper, the wheel power command for the vehicle to follow the US06 cycle is saturated to non-negative values and we use this saturaed profile (see Fig. 4 for an example) for the controller gain optimization.

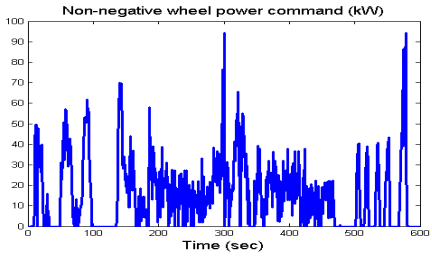

Fig. 4. The saturated non-negative wheel power command for the vehicle with battery 3 (B_s = 2.57e-5) to follow US06 cycle.

The cost function J includes three terms: engine fuel consumption, equivalent fuel consumption from the battery at the end of driving cycle, and accumulated vehicle power tracking error.

$$J = \int_0^{T_f} \dot{m}_{ice}(t)dt + K_{eqf}\left|soc_r - soc_f\right| + \alpha\int_0^{T_f}\left|P_{w,cmd}(t) - P_w(t)\right|dt \tag{8}$$

where: $\dot{m}_{ice}(t)$ represents the engine fuel consumption; $soc_f = soc(T_f)$ is the battery SoC at the end of the driving cycle; K_{eqf} is the equivalent fuel consumption factor from external charge [20]; and α is the penalty weight to drive the power tracking error to zero.

The design variables are the controller gains: k_1, k_2, k_3, n_1, n_2, k_e and k_b. The feedback gains k_4, k_5 and k_6 are calculated from k_1, k_2 and k_3 using equations (7).

The constraints include: 1) stability of the closed loop system with the linear controller, which is enforced by the closed loop pole locations; 2) upper and lower power limits of the engine; 3) limit on engine power rate of change for gradual operation; 4) upper and lower power limits of the battery; 5) upper and lower limits on battery SoC; 6) upper and lower bounds on battery SoC at the end of the driving cycle to enforce charge sustainability.

In order to check the battery charge sustainability, we set the initial SoC in the simulation as the reference SoC, soc_r. Since SoC varies between 0 and 1, a smaller battery needs to have a larger soc_r to satisfy the required battery energy availability requirement for the CS mode [21].

The design results are presented in TABLE III.

TABLE III
SIMULATION RESULTS WITH CENTRALIZED CONTROL

B_s (e-5)	MPG	$err_{p,max}$	$soc_{dev,p}$
1.29	27.58	2.16e-7	-2%
1.71	28.17	8.10e-8	-2%
2.57	28.78	4.65e-8	-2%
5.14	29.40	3.61e-6	-2%

The fuel economy, considering both fuel consumption from the engine and equivalent fuel consumption from the battery at the end of the driving cycle, are evaluated in miles per gallon (MPG). The driving performance is evaluated using the maximum power tracking error $err_{P,max}$ in kW. The

battery charge sustaining performance, $soc_{dev,p}$, is evaluated by the deviation of the final SoC from the reference SoC:

$$soc_{dev,p} = \frac{soc_f - soc_r}{soc_r} \cdot 100\% \tag{9}$$

In the charge sustaining control, MPG increases as the battery size decreases due to the decrease in battery weight. But a larger battery can provide higher fuel economy through extended all-electric range. Therefore, a larger battery will still provide higher overall MPG considering both all-electric range and charge sustaining range [2].

An example power split between the engine and the battery for the vehicle with battery 3 (B_s = 2.57e-5) to follow the saturated US06 cycle is shown in Fig. 5. The engine essentially delivers the moving average of the wheel power command, while the battery provides the transients.

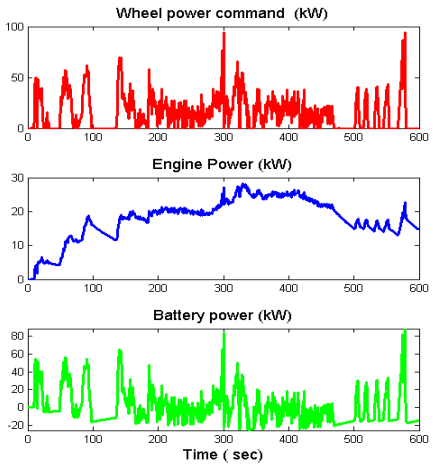

Fig. 5. An example power split between the engine and the battery for the vehicle with battery 3 (B_s = 2.57e-5) over the saturated US06 cycle.

Fig. 6 shows the battery SoC trajectories for each vehicle configuration with the four considered batteries to follow the saturated US06 cycle.

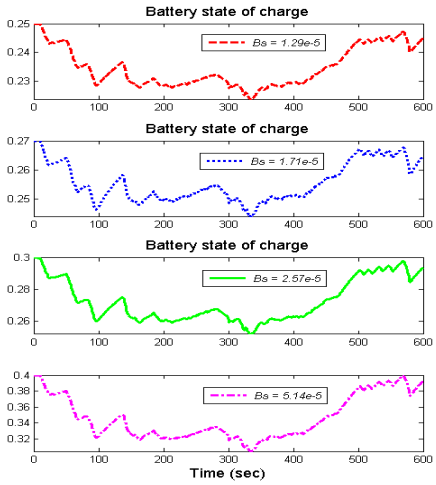

Fig. 6. Battery SoC profiles for each vehicle configuration with different batteries over the saturated US06 cycle.

IV. Distributed Controller for Battery CSM

A distributed supervisory controller for the PHEV is introduced in Fig. 7. The controller is distributed into two parts: the vehicle system controller (VSC), which is fixed with the vehicle, and the battery control unit (BCU), which resides in the battery module and thus is swappable along with the battery. Such an implementation assumes that the battery is a smart component, which has an on-board microcontroller to perform control functions and to communicate with the VSC over a network, see the dashed line in Fig. 7. Other implementations are also possible, e.g., the VSC and the BCU can be physically distributed to the same module and the BCU software and calibration portions can be "reflashed'' when the battery changes.

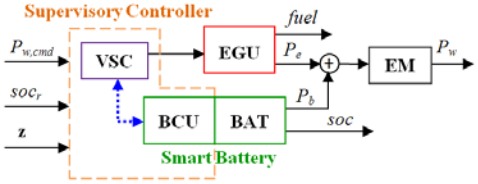

Fig. 7. Diagram of the vehicle components showing the distributed supervisory controller (compared to the centralized controller in Fig. 1).

A. Controller distribution architecture

The controller distribution between the VSC and the BCU addresses the tradeoff between performance (generally highest when the controller is entirely within the BCU) and simplicity of the BCU implementation (desirable in terms of computing and calibration effort). While controller simplicity can be measured in a variety of ways, here we relate controller simplicity to controller order and the number of gains.

The supervisory controller is distributed as follows:
Control functions in the VSC:

$$z_3 = \int (P_{w,cmd} - P_w)dt$$

$$P_{e,cmd} = k_3 z_3 + n_1 P_{w,cmd} + k_e P_{b,cmd} + P_{be} \tag{10}$$

$$P_{eb} = k_6 z_3 + n_2 P_{w,cmd} + k_b P_{e,cmd} \tag{11}$$

Control functions in the BCU:

$$z_1 = \Delta soc = soc_r - soc$$

$$z_2 = \int (\Delta soc)dt = \int (soc_r - soc)dt$$

$$P_{b,cmd} = k_4 z_1 + k_5 z_2 + P_{eb} \tag{12}$$

$$P_{be} = k_1 z_1 + k_2 z_2 \tag{13}$$

Note that the SoC related calculations are confined to the battery module. The signal paths on the network between the VSC and the BCU are detailed in Fig. 8.

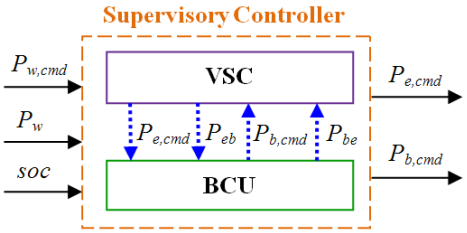

Fig. 8. The signal paths on the network between the VSC and the BCU.

When the battery changes, only the controller gains, k_1, k_2, k_4 and k_5, in the BCU, need to be changed, while the controller gains k_3, k_6, n_1, n_2, k_e and k_b, in the VSC remain the same. The different design freedom of the controller gains necessitates a bi-level optimization formulation to obtain the optimal controller gains.

B. Optimization of the distributed controller gains

Consider n possible batteries, $n = 4$ in our case as given in TABLE II. We denote the controller gains in the VSC as $\mathbf{x}_s$, and the vector of the controller gains in the BCU as $\mathbf{x}_{m,i}$, for each vehicle configuration with battery parameter $B_{s,i}$, $i \in \{1, \ldots, n\}$. We introduce auxiliary variables $\mathbf{x}_{s,i}$, to serve as local copies of the shared controller gains $\mathbf{x}_s$ for the vehicle configuration with battery parameter $B_{s,i}$. The design variables $\mathbf{x}_s$ and $\mathbf{x}_{s,i}$ are forced to be equal by the consistency constraint $\mathbf{c}: R^{(n+1)\cdot m_1} \mapsto R^{n\cdot m_1}$, which is defined as $\mathbf{c}(\mathbf{x}_s, \mathbf{x}_{s,1}, \mathbf{x}_{s,2}, \ldots, \mathbf{x}_{s,n}) = [\mathbf{c}_1^T, \mathbf{c}_2^T, \ldots, \mathbf{c}_n^T]^T = \mathbf{0}$, with $\mathbf{c}_i(\mathbf{x}_s, \mathbf{x}_{s,i}) = \mathbf{x}_s - \mathbf{x}_{s,i}$, where $\mathbf{c}_i \in R^{m_1}$ is the vector of consistency constraints for the vehicle configuration with battery parameter $B_{s,i}$, and m_1 is the dimension of $\mathbf{x}_s$.

The consistency constraints are relaxed by an augmented lagrangian penalty function $\phi: R^{n\cdot m_1} \mapsto R$.

$$\phi(\mathbf{c}) = \mathbf{v}^T\mathbf{c} + \|\mathbf{w} \circ \mathbf{c}\|_2^2 = \sum_{i=1}^{n} \phi_i(\mathbf{c}_i(\mathbf{x}_s, \mathbf{x}_{s,i})) \tag{14}$$

with the penalty function for each system configuration with component parameter $B_{s,i}$, $\phi_i: R^{m_1} \mapsto R$ defined by:

$$\phi_i(\mathbf{c}_i(\mathbf{x}_s, \mathbf{x}_{s,i})) = \mathbf{v}_i^T(\mathbf{x}_s - \mathbf{x}_{s,i}) + \|\mathbf{w}_i \circ (\mathbf{x}_s - \mathbf{x}_{s,i})\|_2^2 \tag{15}$$

where $\mathbf{v} = [\mathbf{v}_1^T, \mathbf{v}_2^T, \ldots, \mathbf{v}_n^T]^T \in R^{n\cdot m_1}$ is the vector of Lagrange multiplier estimates for the consistency constraints; and $\mathbf{w} = [\mathbf{w}_1^T, \mathbf{w}_2^T, \ldots, \mathbf{w}_n^T]^T \in R^{n\cdot m_1}$ is the vector of penalty weights. The symbol $\circ$ represents the Hadamard product: an entry-wise vector multiplication.

The outer stage optimization minimizes the penalty function with respect to the controller gains in the VSC, $\mathbf{x}_s$:

$$\phi(\mathbf{c}) = \sum_{i=1}^{n} \phi_i(\mathbf{c}_i(\mathbf{x}_s, \mathbf{x}_{s,i})) \tag{16}$$

Note that the outer stage problem has no constraints. It can be solved analytically:

$$\mathbf{x}_s^* = \arg\min_{\mathbf{x}_s} \phi(\mathbf{c}) = \frac{\sum_{i=1}^{n}(\mathbf{w}_i \circ \mathbf{w}_i \circ \mathbf{x}_{s,i}) - \frac{1}{2}\sum_{i=1}^{n}\mathbf{v}_i}{\sum_{i=1}^{n}(\mathbf{w}_i \circ \mathbf{w}_i)} \tag{17}$$

In the inner stage optimization for each battery application with $B_{s,i}$, the objective function includes two terms, the cost function J as defined in equation (8), and the penalty function as defined in equation (15).

$$\min \; J(\mathbf{x}_{s,i}, \mathbf{x}_{m,i}, B_{s,i}) + \phi_i(\mathbf{c}_i(\mathbf{x}_s, \mathbf{x}_{s,i}))$$

The design variables of each inner stage optimization are the auxiliary variables, $\mathbf{x}_{s,i}$ and the controller gains in the BCU, $\mathbf{x}_{m,i}$. The relaxation errors between $\mathbf{x}_{s,i}$ and $\mathbf{x}_s$ are driven to zero by the penalty function. The constraints for each battery application are the same as described in Section III. The inner stage problems can be solved using nonlinear programming methods.

The flowchart of the solution algorithm is illustrated in Fig. 9. The design variables of the outer stage, $\mathbf{x}_s$, are fixed parameters for each of the inner stage problems. At each iteration, a new estimate of $\mathbf{x}_s$ is generated and each of the inner stage problems is solved using $\mathbf{x}_s$ as a parameter. By appropriate selection of the penalty weights $\mathbf{v}$ and $\mathbf{w}$, the penalty function can be driven to zero for consistency of $\mathbf{x}_s$ and $\mathbf{x}_{s,i}$. The method of multipliers is used to update the penalty weights [22]. At each iteration of the outer stage problem, $\mathbf{v}$ and $\mathbf{w}$ are updated to reduce the relaxation error. This procedure is repeated until a feasible solution that satisfies the consistency constraints $\mathbf{c} < \boldsymbol{\varepsilon}$, for each inner stage optimization is found, or until the maximum number of function evaluations is reached, where $\boldsymbol{\varepsilon}$ is the error tolerance.

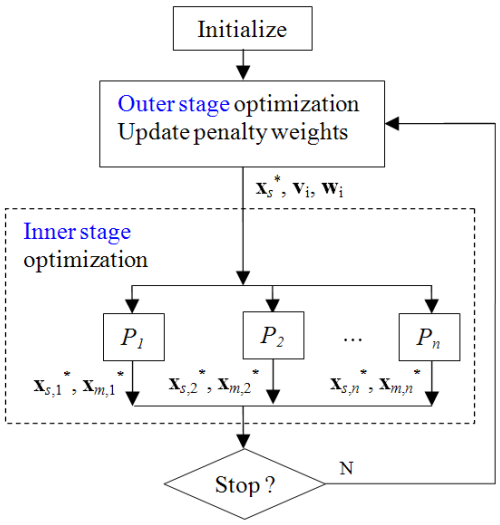

Fig. 9. Flowchart of the solution algorithm.

A good initial guess is important for this bi-level optimization problem, and the design results from the centralized controller can be employed.

The resulting controller gains in the VSC are: $[k_3, n_1, k_e, n_2, k_b] = [1.82, 0.01, 0.06, 1.23, 0.05]$. The VSC is the same for different battery applications.

The controller gains in the BCU for each battery are listed in TABLE IV. The performance metric for the distributed controller are also listed in TABLE IV.

TABLE IV
SIMULATION RESULTS WITH DISTRIBUTED CONTROL

B_s(e-5)	k_1	k_2	MPG	$err_{p,max}$	$soc_{dev,p}$
1.29	917.42	1.59	27.58	6.18e-4	-2%
1.71	1000	1.34	28.16	6.02e-4	-2%
2.57	466.87	0.93	28.78	5.82e-4	-2%
5.14	222.23	0.50	29.40	5.54e-4	-2%

The driving performance in terms of wheel power tracking error and battery charge sustaining are satisfied with either centralized control or distributed control, as shown in TABLEs III and IV. Note that the distributed controller achieves battery CSM without sacrificing fuel economy versus the centralized control case. At the same time, the BCU is reasonably simple and can be implemented with a modest on-board microcontroller in the battery module. As the controller functionality related to the battery SoC are confined to the BCU, the estimation of battery SoC (not considered in this paper) can be confined to the BCU as well, making the battery module functionally independent both in hardware and software (i.e., control algorithms).

V. SUMMARY AND CONCLUSIONS

In this paper, we proposed a method for distributed controller design to achieve battery CSM in PHEVs. This method generates the distributed controller gains by solving a bi-level optimization problem using the augmented lagrangian decomposition method. The simulation results indicate that battery CSM can be achieved without compromising fuel economy compared to the centralized control case. With the proposed distributed controller, the battery module can be swapped without redesign or recalibration of the system level controller. In other words, the battery module becomes a plug and play component, and the system performance is automatically configured to be optimal for each battery application.

The above results and conclusions are based on a PHEV model and controller that do not include regenerative braking. The extension of the designs to include regenerative braking will be reported in future publications.

REFFERENCES

[1] A.A. Pesaran, T. Markel, H. S. Tataria, and D. Howell, "Battery Requirements for Plug-In Hybrid Electric Vehicles – Analysis and Rationale," *Conference Paper, NREL/CP-540-42240,* pp. 1-12, 2009.

[2] T. Markel and A. Simpson, "Plug-In Hybrid Electric Vehicle Energy Storage System Design," *Conference Paper, NREL/CP-540-39614,* pp. 1-9, 2006.

[3] M. Cakmakci and A. G. Ulsoy, "Improving Component-Swapping Modularity Using Bidirectional Communication in Networked Control System," *IEEE/ASME Transactions on Mechatronics,* vol. 14, pp. 307 - 316 2009.

[4] A. G. Michelsen and J. Stoustrup, "High level model predictive control for plug-and-play process control with stability guaranty," *Proceedings of the 49th IEEE Conference on Decision and Control,* 2010.

[5] J. P. Hespanha, P. Naghshtabrizi, and Y. Xu, "A survey of recent results in networked control systems," *Proceedings of the IEEE,* vol. 95, pp. 138-172, 2007.

[6] M. Cakmakci and A. G. Ulsoy, "Swappable distrituted MIMO controller for a VCT engine," *IEEE Transactions on Control System Technology (in press)*.

[7] S. Li, M. Cakmakci, I. V. Kolmanovsky, and A. G. Ulsoy, "Throttle actuator swapping modularity design for idle speed control " *Proceedings of American Control Conference,* pp. 2702-2707, 2009.

[8] S. Li, Ilya V. Kolmanovsky, and A. G. Ulsoy, "Direct optimal distributed controller design for component swapping modularity with application to ISC," *Proceedings of American Control Conference,* pp. 5368-5373, 2010.

[9] S. Li, I. V. Kolmanovsky, and A. G. Ulsoy, "Direct optimal distributed controller design for component swapping modularity with application to ISC," *Proceedings of American Control Conference,* pp. 5368-5373, 2010.

[10] S. Tosserams, L. F. P. Etman, and J. E. Rooda, "An augmented Lagrangian decomposition method for quasi-separable problems in MDO," *Structural and Multidisciplinary Optimization,* vol. 34, pp. 211-227, 2007.

[11] S. G. Wirasingha and A. Emadi, "Classification and review of control strategies for plug-In hybrid electric vehicles," *Vehicular Technology, IEEE Transactions on,* vol. 60, pp. 111-122, 2011.

[12] W. Jong-Seob, R. Langari, and M. Ehsani, "An energy management and charge sustaining strategy for a parallel hybrid vehicle with CVT," *Control Systems Technology, IEEE Transactions on,* vol. 13, pp. 313-320, 2005.

[13] G. Paganelli, S. Delprat, T. M. Guerra, J. Rimaux, and J. J. Santin, "Equivalent consumption minimization strategy for parallel hybrid powertrains," *IEEE 55th Vehicular Technology Conference,* pp. 2076-2081, 2002.

[14] L. Chan-Chiao, P. Huei, J. W. Grizzle, and K. Jun-Mo, "Power management strategy for a parallel hybrid electric truck," *Control Systems Technology, IEEE Transactions on,* vol. 11, pp. 839-849, 2003.

[15] Edward Dean Tate Jr, J. W. Grizzle, and H. Peng, "Shortest path stochastic control for hybrid electric vehicles," *Int. J. Robust Nonlinear Control,* pp. 1409–1429, 2008.

[16] A. Konev, L. Lezhnev, and I. Kolmanovsky, "Control strategy optimization for a series hybrid vehicle " *SAE paper 2006-01-0663,* 2006.

[17] S. Di Cairano, W. Liang, I. Kolmanovsky, M. L. Kuang, and A. M. Phillips, "Engine power smoothing energy management strategy for a series hybrid electric vehicle," *Proceedings of the American Control Conference,* 2011.

[18] T. Markel, A. Brooker, T. Hendricks, V. Johnson, K. Kelly, B. Kramer, M. O'Keefe, S. Sprik, and K. Wipke, "ADVISOR: a systems analysis tool for advanced vehicle modeling," *Journal of Power Sources,* vol. 110, pp. 255-266, 2002.

[19] J.-F. Magni, S. Bennani, J. Terlouw, L. Faleiro, J. de la Cruz, and S. Scala, "Eigenstructure assignment," *Robust Flight Control, Springer Berlin / Heidelberg,* pp. 22-32, 1997.

[20] "Code of Federal Regulations 474.3," *http://cfr.vlex.com/source/code-federal-regulations-energy-059,* 2005.

[21] S. Li, "Distributed supervisory controller design for battery swapping modularity in plug-in hybrid electric vehicles," *Doctoral dissertation, Univerity of Michigan,* 2011.

[22] D. P. Bertsekas, *Nonlinear programming*. Belmont, Masssachusetts: Athena Scientific, 2003.